AIAA JOURNAL
Vol. 30, No. 8, August 1992

Performance of Popular Turbulence Models for Attached and Separated Adverse Pressure Gradient Flows

F. R. Menter*
Eloret Institute, Palo Alto, California 94303

The performance of four popular eddy-viscosity turbulence models under adverse pressure gradient conditions is investigated. The Baldwin-Lomax, Johnson-King, Baldwin-Barth, and Wilcox k-ω models have been implemented into the INS code, which solves the incompressible Reynolds-averaged Navier-Stokes equations. Results will be shown for the well-known Samuel-Joubert flow and two new flowfields, recently reported by D. M. Driver. The two new flowfields pose a stronger test of the models than does the Samuel-Joubert flow because of the more severe retardation of the boundary layer, including separation in one case. A detailed comparison of the numerical results and the experimental data will be shown.

Introduction

INCREASING computer capacity and the development of efficient numerical methods allow the solution of the Reynolds-averaged Navier-Stokes equations for practical aerodynamic applications. Of crucial importance for the accuracy of the results is the performance of the turbulence model. With the increasing complexity of the flows under investigation, the demand for reliable turbulence models is as high as ever.

Of special importance for engineering applications is the accurate prediction of adverse pressure gradient flows with and without separation. It was one of the conclusions of the AFOSR-HTTM Stanford Conference in 1981[1] that most of the turbulence models at that time had significant problems in predicting even the simplest of these flows. Since then several new approaches have been proposed,[2-4] and some have led to considerable improvements in aerodynamic predictions.

The importance of these flows is also confirmed by new experimental investigations. Driver[5] recently reported detailed measurements for two adverse pressure gradient flows. In his experiment, a turbulent boundary layer develops in the axial direction along a circular cylinder. Two different pressure distributions have been produced by diverging wind-tunnel walls and applying suction at these walls. One of his flow cases remains attached, whereas the other one is separated.

The availability of new experimental data led to the investigation of the performance of some of the more popular models under different adverse pressure gradients. The Navier-Stokes method of Rogers and Kwak,[6] which solves the incompressible Navier-Stokes (INS) equations, has been adopted for the present study. To put the results into the context of previous investigations, the well-known flow of Samuel and Joubert[7] was also computed. The results of the computations will be compared with each other and against the experimental data.

Presented as Paper 91-1784 at the AIAA 22nd Fluid Dynamics, Plasma Dynamics, and Lasers Conference, Honolulu, HI, June 24-26, 1991; received Aug. 26, 1991; revision received Jan. 23, 1992; accepted for publication Jan. 25, 1992.

*Research Engineer, 3788 Fabian Way; mailing address, NASA Ames Research Center, Mail Stop 229-1, Moffett Field, CA 94035-1000.

Turbulence Models

The investigation covers the following range from zero- to two-equation eddy-viscosity models:

1) Baldwin-Lomax (BL) model (zero-equation model)[8]
2) Johnson-King (JK) model (half-equation model)[9,10]
3) Baldwin-Barth (BB) model (one-equation model)[3]
4) Wilcox model (k-ω) (two-equation model).[11]

All of the models except the BB model are applied in the latest version proposed by the corresponding authors. For the BB model the originally proposed model[3] gave significantly better results than the modified formulation.[12] It was therefore decided to use the original equations.

The BL model is mainly used for reference purposes, since it is still used in many of the existing Navier-Stokes methods. The other three models have been chosen because they have shown promising results so far but have not been compared extensively with experimental data.

The JK model has led to a considerable improvement of numerical predictions for transonic airfoil flows. This improvement is mainly the result of the solution of an ordinary differential equation for the maximum turbulent shear stress, which controls the level of the eddy viscosity in the outer part of the boundary layer. The formulation for the inner eddy viscosity has recently been modified by Johnson and Coakley[10] in order to account for the small logarithmic region near the wall in adverse pressure gradient flows.

The BB model has a significant advantage over the BL and JK models in that no length scale has to be specified. This, in conjunction with the fact that only one partial differential equation must be solved, makes the model attractive from a numerical point of view. Since the model has only recently been proposed, its performance under complex flow situations has yet to be assessed.

The k-ω model of Wilcox was chosen for two reasons. First, it gave superior results for the adverse pressure gradient flows

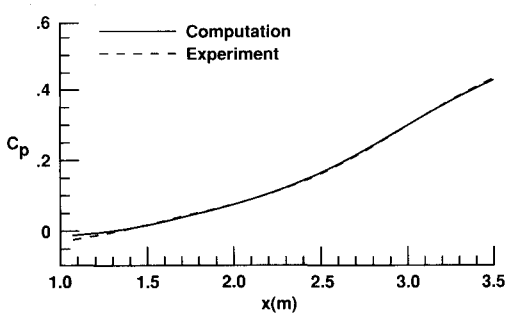

Fig. 1 Comparison of computed and measured wall pressure distributions for Samuel-Joubert flow.

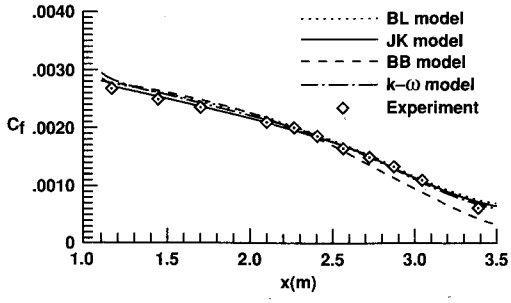

Fig. 2 Comparison of computed and measured wall shear-stress distributions for Samuel-Joubert flow.

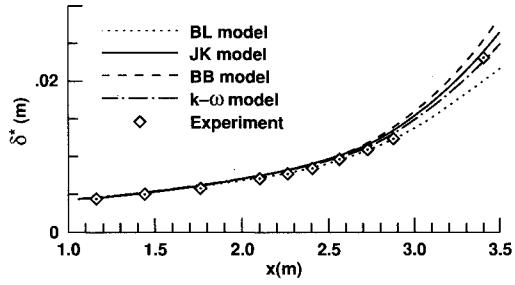

Fig. 3 Comparison of computed and measured displacement thicknesses for Samuel-Joubert flow.

computed by Wilcox[11] when compared with other two-equation models. Second, because of its mathematical simplicity, it does not need damping functions in the low Reynolds number region close to the wall, and the ω equation has an exact boundary condition at the wall. Of specific interest is the behavior of this model in the case of separated flow, since no detailed comparison with separated flow data has yet been reported.

A detailed description of all models is given in Ref. 13 and is therefore not repeated here.

Numerical Method

The computations have been performed with the numerical method developed by Rogers and Kwak.[6] It solves the incompressible, Reynolds-averaged Navier-Stokes equations using the method of pseudocompressibility. The equations can be solved in a time-accurate or pseudotime manner. Since the investigated flows are all steady in the mean quantities, the second approach was chosen. The convective terms are discretized with a third-order upwind-difference scheme based on flux-difference splitting. The resulting algebraic equations are solved with an implicit line-relaxation scheme.

The partial differential equations (PDE) for the turbulence quantities have been solved decoupled from the mean flow equations. At every pseudotime step, the equations for the mean flow and subsequently the equations for the turbulence variables have been solved. The convection terms in the turbulence transport equations were discretized with the same third-order upwind scheme used for the mean flow equations.

The Samuel-Joubert flow was computed with the two-dimensional version of the code (INS2D). A grid of 90×90 points was used for these computations. Since the k-ω model is believed to be the most sensitive with regard to the grid spacing, the computations with this model have been repeated on a 60×60 grid, and only minor changes in the solution could be found.

The two flowfields of Driver[5] have a rotational symmetry that cannot be accounted for in INS2D. It was therefore necessary to compute them with the three-dimensional version of the code (INS3D). However, only three planes had to be used in the circumferential direction because of the symmetry conditions. The two side planes were closely spaced around the middle plane to avoid numerical inaccuracies introduced by the boundary conditions. Most of the computations have been performed both on a $60 \times 3 \times 60$ and a $40 \times 3 \times 80$ grid. The computations with the k-ω model have also been repeated on a $100 \times 3 \times 100$ grid. Again, no significant grid dependence could be found.

Results and Discussion

The flowfield of Samuel and Joubert is described in detail in Ref. 7. It is a flat plate boundary-layer flow developing under

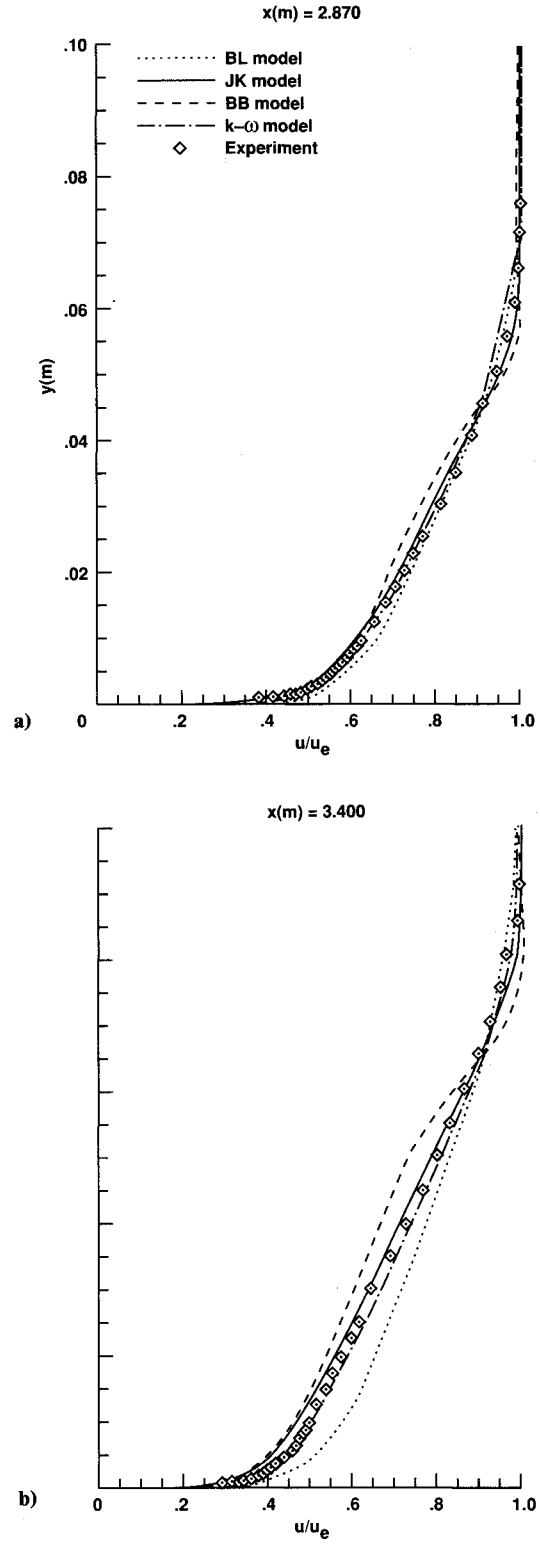

Fig. 4 Comparison of computed and measured velocity profiles for Samuel-Joubert flow.

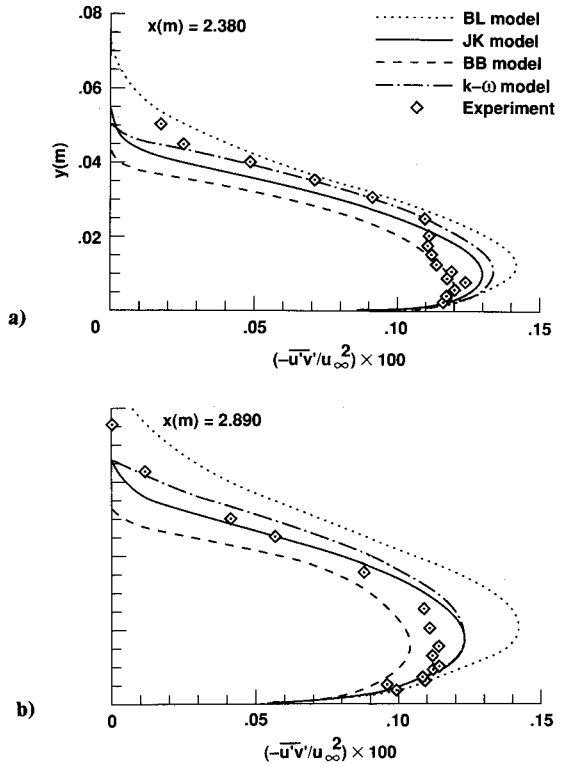

Fig. 5 Comparison of computed and measured shear-stress profiles for Samuel-Joubert flow.

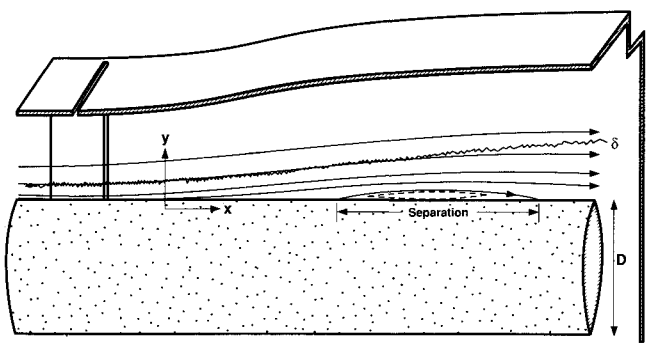

Fig. 6 Experimental setup for adverse pressure gradient flows for cases BS0 and CS0 of Driver.[5]

an increasingly adverse pressure gradient. The freestream Reynolds number is 1.7×10^6 m^{-1}. The flow is retarded by the pressure gradient, but it does not separate. For the computations the experimental wall pressure was specified at the outer edge of the computational domain. Figure 1 shows that the computed and the measured wall pressures are almost identical, which justifies the use of this boundary condition.

Figure 2 shows a comparison of the computed and the measured wall shear-stress distributions. All models give reasonable results, with the best agreement found for the JK model. Note that the c_f values for the k-ω model are slightly higher than those reported by Wilcox.[11] This may be due to slightly different initial conditions. It was found that the results are rather sensitive to the inlet conditions specified for k. For the present computations the inflow values of k and ω were chosen to match the experimental shear-stress and turbulent kinetic energy profiles. The velocity profile was also specified from the experiments.

Figure 3 shows a comparison of the displacement thicknesses δ^*. The BL model underestimates the displacement effect, whereas the BB model gives too high values for δ^*. This can also be inferred from the predicted velocity profiles that are shown for two axial locations in Fig. 4.

A comparison of computed and measured turbulent shear-stress profiles is shown in Fig. 5. The rapid descent of the shear stress toward the boundary-layer edge for the BB model leads to the pronounced curvature of the velocity profiles in this region seen in Fig. 4. It should be noted that the modifications introduced in Ref. 12 are designed to increase the diffusion terms to overcome this problem. However, the modified version leads to velocity profiles (not shown) even fuller than the one obtained with the BL model and therefore to a severe underestimation of the displacement effect.

The other two flowfields investigated have recently been reported by Driver.[5] Figure 6 shows a schematic of the experimental setup. A turbulent boundary layer develops in the axial direction of a circular cylinder. Adverse pressure gradients can be produced with the help of diverging wind-tunnel walls and suction applied at these walls. Two different adverse gradient flows have been studied. The milder pressure increase of the first case, BS0, leaves the flow attached, whereas the pressure distribution of the second case, CS0, leads to separation. Driver reports measurements of wall shear-stress and wall pressure distributions, mean flow velocity profiles, and second- and third-order correlations of the fluctuating velocities. Measurements of the c_f and c_p distributions at different circumferential locations were used to verify the rotational symmetry of the flow. The inflow Reynolds number for both flows, based on the diameter D of the cylinder is $Re = 2.8 \times 10^5$.

The boundary conditions for the computations were specified as follows. At the inflow boundary the experimental velocity profile was given. The inflow eddy viscosity was computed from the equilibrium JK model. (For the BL model the BL eddy viscosity was used.) For the k-ω model the second inflow condition was $k = \overline{(-u'v')}/0.3$. At the wall the usual no-slip conditions were applied. At the outer boundary an inviscid streamline was specified. The shape of this streamline was computed from the measured displacement effect of the boundary layer. Note that this does not mean that the displacement thickness is specified, since the pressure can adjust freely. At the outflow, zero-gradient conditions were given.

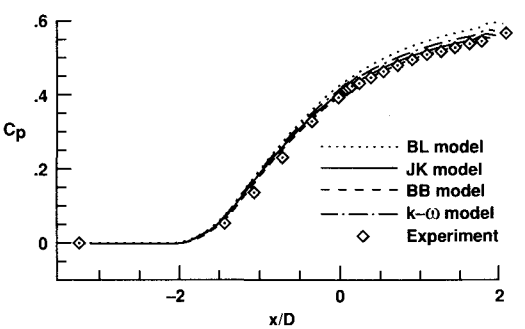

Fig. 7 Comparison of computed and measured wall pressure distributions for case BS0.

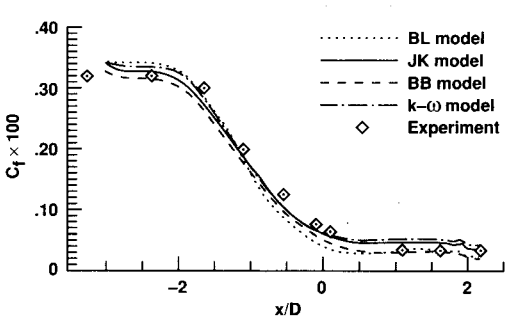

Fig. 8 Comparison of computed and measured wall shear-stress distributions for case BS0.

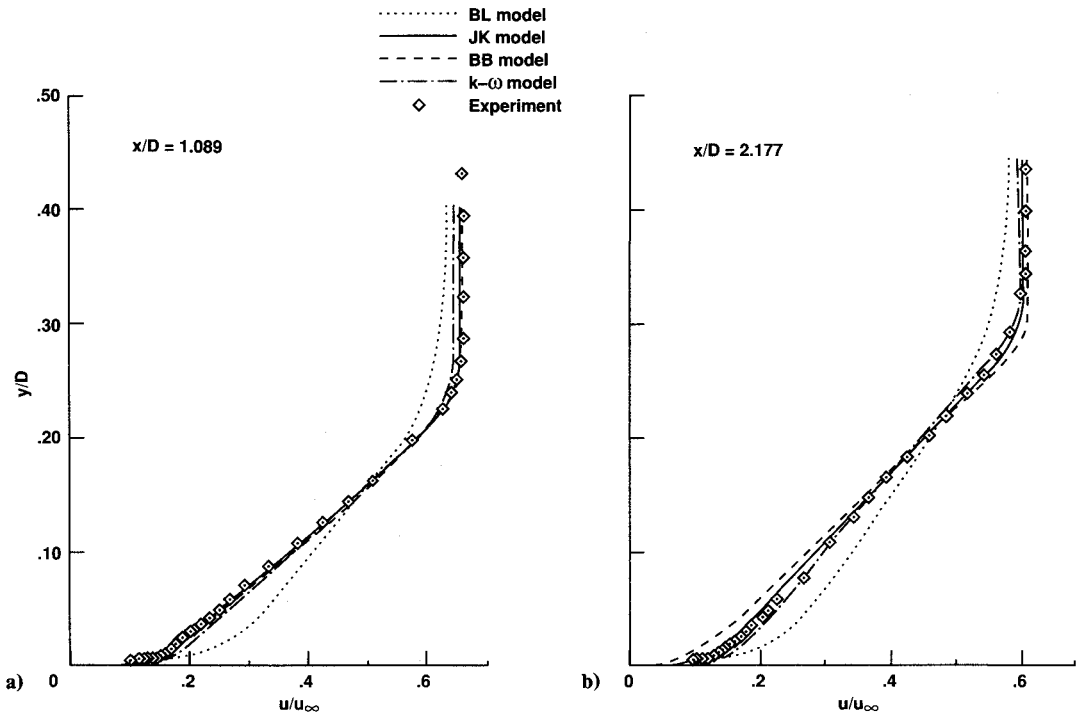

Fig. 9 Comparison of computed and measured velocity profiles for case BS0.

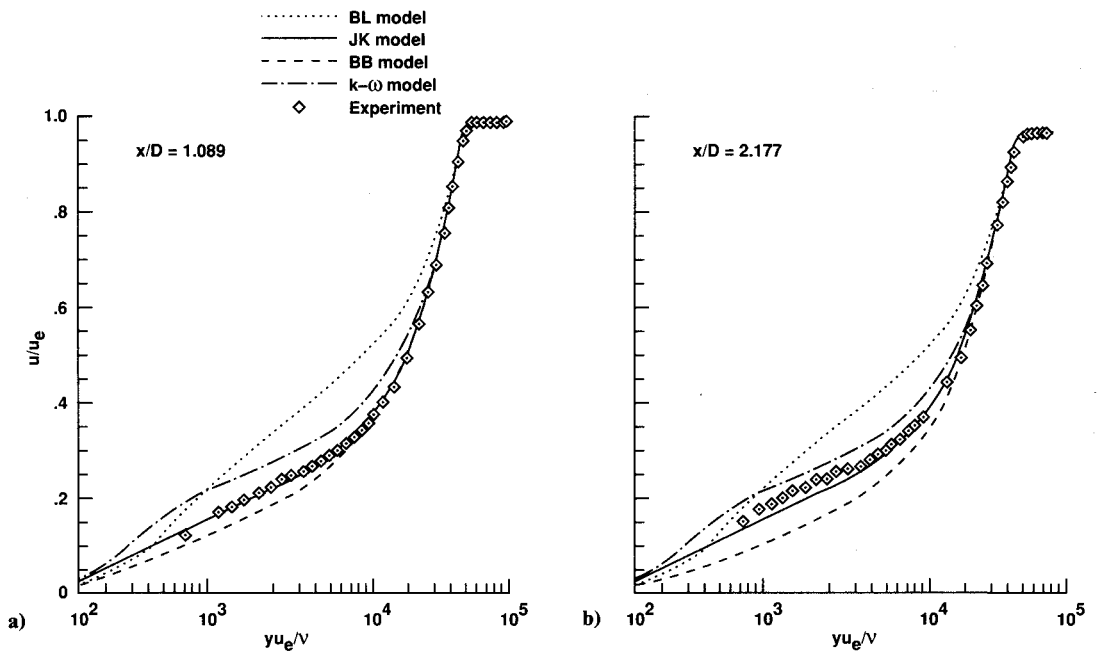

Fig. 10 Comparison of computed and measured velocity profiles for case BS0 in semilogarithmic scale.

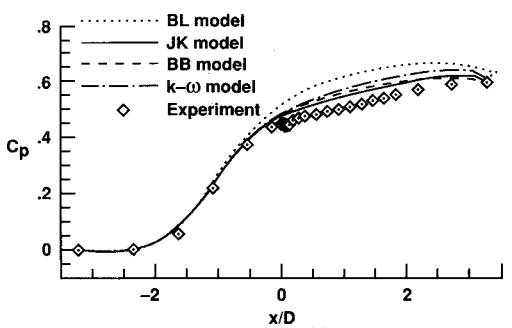

Fig. 11 Comparison of computed and measured wall pressure distributions for case CS0.

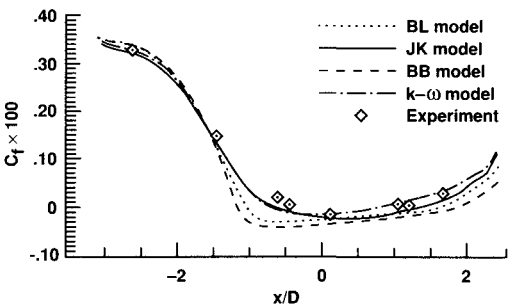

Fig. 12 Comparison of computed and measured wall shear-stress distributions for case CS0.

Even for the milder case, BS0, the retardation is more severe than for the Samuel-Joubert flow. The shape factor varies between 1.3 and 2.0, whereas the variation for the Samuel-Joubert flow is only between 1.3 and 1.6.

Figures 7 and 8 show the wall pressure and the wall shear-stress distributions, respectively, for case BS0. The c_p distribution is reproduced with good accuracy by the three nonequilibrium models. The BL model gives somewhat higher c_p values, which is again an indication that the displacement effects are underestimated. Note that the wall shear-stress values have not been measured independently for case BS0 but were obtained from the measured velocity profiles.

Figure 9 shows a comparison of the velocity profiles for this case. The differences between the profiles are similar to the ones observed for the Samuel-Joubert flow. The best results were produced by the JK and the k-ω models. The BL model fails to predict the retardation in the near-wall region correctly and therefore produces incorrect profile shapes. The BB model gives significantly better results than for the Samuel-Joubert flow. However, some differences appear near the boundary-layer edge at $x/D = 2.177$.

Differences in the near-wall region can be seen more clearly in the logarithmic scale of Fig. 10. It is interesting to note that all models give similar c_f distributions (Fig. 8) in spite of the large differences of the velocity profiles in the near-wall region.

The last flow investigated is the case CS0 of Driver. A stronger divergence of the wind-tunnel walls (plus suction at these walls) leads to a separated flowfield. Figures 11 and 12 show the c_p and c_f distributions. The strong retardation leads to larger displacement effects, reflected in a flattening of the experimental c_p distribution. All models underestimate this effect but do so by different magnitudes. The worst results are obviously obtained with the BL model. Note that tests with other equilibrium models, such as the Cebeci-Smith model, gave similar results.

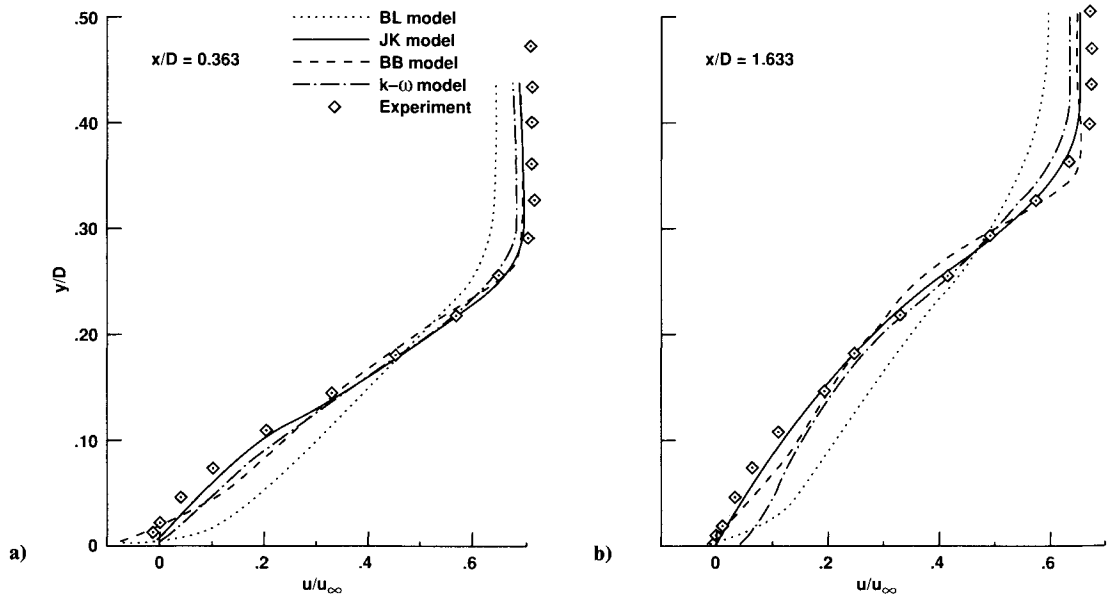

Fig. 13 Comparison of computed and measured velocity profiles for case CS0.

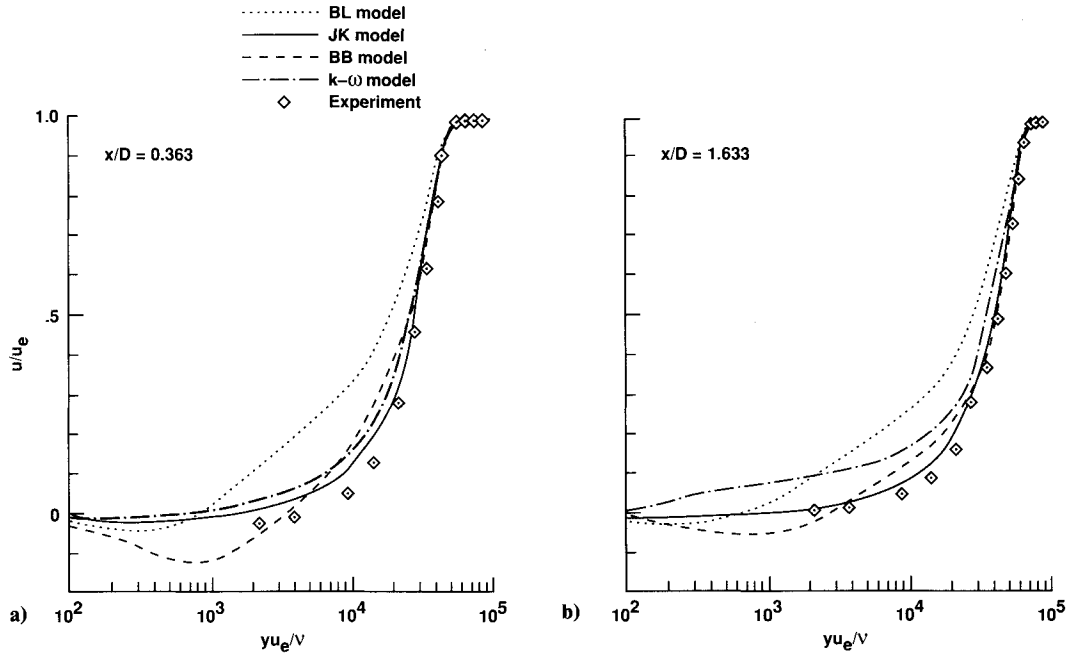

Fig. 14 Comparison of computed and measured velocity profiles for case CS0 in semilogarithmic scale.

Large differences between the models can also be found in the c_f distributions (for this case the wall shear stress was measured independently by the oil-film interferometer technique). The JK model gives values rather close to the experiment. The k-ω model is also rather close but underestimates the length of the separation zone. The other two models predict separation too early and extend it too far downstream.

The differences can be seen more clearly in Figs. 13 and 14, which show the velocity profiles in linear and logarithmic scales, respectively. The BB model predicts a thin separation zone and almost no displacement effect. The BB model shows a behavior similar to that for the Samuel-Joubert flow. It exaggerates the wake region and gives incorrect profile shapes close to the wall. The JK model gives the best predictions, with only a slight underprediction of the amount of retardation. The k-ω model also gives physically correct profile shapes but underpredicts retardation more than the JK model.

The reason for this can be seen in the turbulent shear-stress profiles shown in Fig. 15. It was found in all of the computations with different versions of the JK and the k-ω model that very accurate velocity profiles could be obtained when the shear-stress profiles near separation were predicted correctly. The larger the maximum shear stress is in this region, the less is the displacement effect farther downstream. Since the k-ω model predicts higher shear-stress values than the JK model does, it underpredicts separation. See also Fig. 16, which

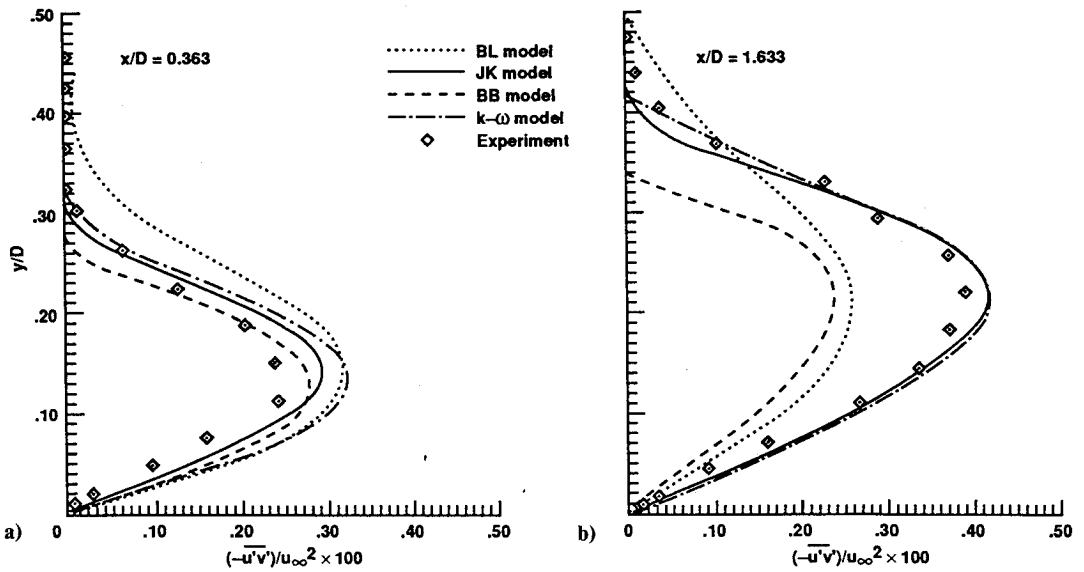

Fig. 15 Comparison of computed and measured shear-stress profiles for case CS0.

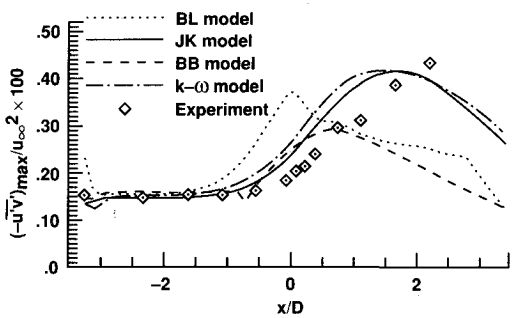

Fig. 16 Development of the maximum turbulent shear-stress vs x/D for case CS0.

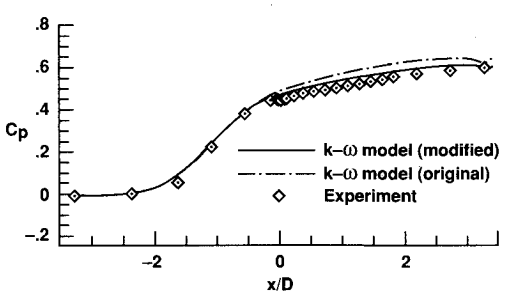

Fig. 18 Comparison of the wall pressure distribution for the original and the modified k-ω model (case CS0).

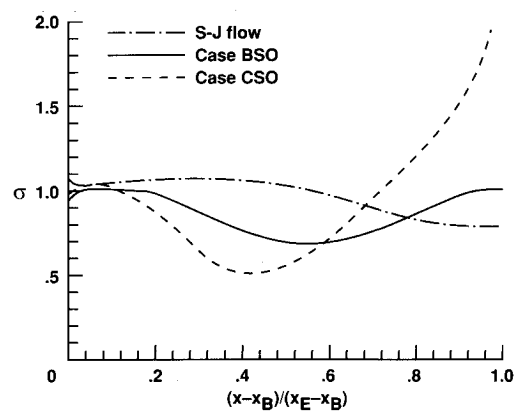

Fig. 17 Nonequilibrium factor $\sigma(x)$ of the Johnson-King model for three different flows.

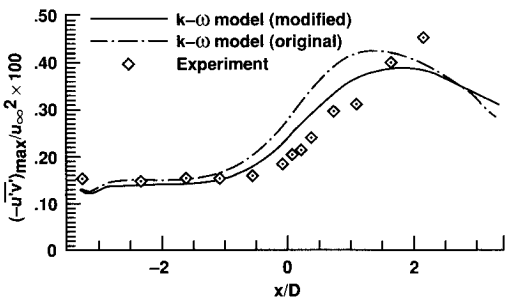

Fig. 19 Comparison of the development of the maximum turbulent shear stress vs x/D for the original and the modified k-ω model (case CS0).

shows the evolution of the maximum turbulent shear-stress vs x/D. The JK and the k-ω models produce obviously similar results, with the JK model being closer to the experiments.

The nonequilibrium factor $\sigma(x)$ that appears in the formulation of the outer eddy viscosity in the JK model [Eq. (3) in Ref. 9] is plotted for all three flows in Fig. 17. The eddy viscosity for the Samuel-Joubert (SJ) flow is not very different from the equilibrium model for a large part of the flowfield, which implies that transport effects are not very important. The large variation of $\sigma(x)$ for the other two cases shows that the advection terms are important not only in compressible flows, where strong variations occur through shock waves, but also in the present incompressible applications.

Some final comments on the behavior of the k-ω model follow. It is well known that the k-ϵ model, from which the k-ω model was derived, produces unacceptably high shear-stress levels in adverse pressure gradient flows. This is usually attributed to the ϵ equation, and various modifications have been proposed to improve matters.[4,14] However, for a boundary-layer flow outside the viscous sublayer, the equation for the turbulent shear-stress

$$\overline{-u'v'} = c_\mu \frac{k^2}{\epsilon}\frac{\partial u}{\partial y} = \frac{k}{\omega}\frac{\partial u}{\partial y} \tag{1}$$

can be rewritten to give

$$\overline{-u'v'} = \sqrt{\frac{\text{Production}_k}{\text{Dissipation}_k}}\, a_1 k \tag{2}$$

For an equilibrium boundary layer, the ratio of production to dissipation is close to one in the outer part of the layer, and therefore $\overline{-u'v'} = a_1 k$. For an adverse pressure gradient flow this ratio can be significantly larger than one. Driver[5] has shown from his experimental data that for the CS0 case it can be as large as two. Since there is no indication that the ratio of $\overline{-u'v'}/k$ increases to values higher than $a_1 = 0.3$ under an adverse pressure gradient (in fact it decreases), it is clear that Eqs. (1) and (2) give values significantly too high for the turbulent shear stress, even if the kinetic energy and the dissipation rate are computed correctly. The previous argument is also true for the k-ω model and may explain the high values of $\overline{-u'v'}$.

All three flowfields have been recomputed with the following restriction on the eddy viscosity:

$$\nu_t = \min\left[\frac{k}{\omega}, \frac{a_1 k}{(\partial u/\partial y)}\right] \tag{3}$$

with $a_1 = 0.3$. The numerical predictions for all three cases were improved considerably by this manipulation. Figures 18 and 19 show as an example the computed c_p and $\overline{-u'v'}_{\max}$ distributions, respectively, for the separated case in comparison with the original results. Equation (3) has not been sufficiently tested to be recommended for general use (where $\partial u/\partial y$ would have to be replaced by an invariant quantity, like the absolute value of the vorticity), but it shows that the definition $\nu_t = c_\mu k^2/\epsilon$ (or $\nu_t = k/\omega$) is at least as large a source of errors in adverse pressure gradient flows as the ϵ (ω) equation.

Conclusions

The performance of four turbulence models has been tested under adverse pressure gradient conditions. The investigation covered the range from algebraic to two-equation eddy viscosity models. The well-known adverse pressure gradient flow of Samuel and Joubert as well as two recently reported flows of Driver have been computed. The model equations were solved together with the Reynolds-averaged Navier-Stokes equations.

The most obvious conclusion is that the three transport models gave significantly better results than the algebraic BL model did.

The JK model gave the best overall agreement with the experiments. It predicts the turbulent shear stress and the shape of the velocity profiles with the highest accuracy. In the present version it has, however, a tendency to give somewhat high maximum shear-stress levels.

The BB model predicted the displacement effects (and therefore the c_p distributions) with good accuracy. However, the model tends to predict incorrect profile shapes, both in the wake and in the near-wall region. The wall shear-stress distributions are similar to the ones produced by the BL model.

The k-ω model gave more realistic velocity profiles but consistently produced values that were too high for the turbulent shear stress. All other differences with regard to the experiments seem to be related to this single point. The source of this shortcoming seems to be the constitutive relation for the eddy viscosity, which does not account for the advection of the shear stresses. A simple fix to the model improved the results significantly.

Acknowledgments

This research was supported by a grant from NASA to Eloret Institute (NCC2-452). The author wants to thank D. A. Johnson, D. M. Driver, and T. J. Coakley of NASA Ames Research Center for their invaluable help during this study.

References

[1]Kline, S. J., Cantwell, B. J., and Lilley, G. M. (eds.), *1980-1981 AFOSR-HTTM-Stanford Conference on Complex Turbulent Flows: Comparison of Computation and Experiment,* Stanford Univ., Stanford, CA, 1981.

[2]Johnson, D. A., and King, L. S., "A Mathematically Simple Turbulence Closure Model for Attached and Separated Turbulent Boundary Layers," *AIAA Journal,* Vol. 23, No. 11, 1985, pp. 1684–1692.

[3]Baldwin, B. S., and Barth T. J., "A One-Equation Turbulence Transport Model for High Reynolds Number Wall-Bounded Flows," NASA TM-102847, Aug. 1990.

[4]Rodi, W., "Experience with Two-Layer Models Combining the k-ϵ Model with a One-Equation Model near the Wall," AIAA Paper 91-0216, Reno, NV, 1991.

[5]Driver, D. M., "Reynolds Shear Stress Measurements in a Separated Boundary Layer," AIAA Paper 91-1787, 1991.

[6]Rogers, S. E., and Kwak, D., "An Upwind Differencing Scheme for the Time-Accurate Incompressible Navier-Stokes Equations," AIAA Paper 88-2583, Williamsburg, VA, 1988.

[7]Samuel, A. E., and Joubert, P. M., "A Boundary Layer Developing in an Increasingly Adverse Pressure Gradient," *Journal of Fluid Mechanics,* Vol. 66, 1974, pp. 481–505.

[8]Baldwin, B. S., and Lomax, H., "Thin Layer Approximation and Algebraic Model for Separated Turbulent Flows," AIAA Paper 78-257, Huntsville, AL, 1978.

[9]Johnson, D. A., "Transonic Separated Flow Predictions with an Eddy-Viscosity/Reynolds-Stress Closure Model," *AIAA Journal,* Vol. 25, No. 2, 1987, pp. 252–259.

[10]Johnson, D. A., and Coakley T. J., "Improvements to a Nonequilibrium Algebraic Turbulence Model," *AIAA Journal,* Vol. 28, No. 11, 1990, pp. 2000–2003.

[11]Wilcox, D. C., "Reassessment of the Scale-Determining Equation for Advanced Turbulence Models," *AIAA Journal,* Vol. 26, No. 11, 1988, pp. 1299–1310.

[12]Baldwin, B. S., and Barth T. J., "A One-Equation Turbulence Transport Model for High Reynolds Number Wall-Bounded Flows," AIAA Paper 91-0610, Reno, NV, 1991.

[13]Menter, F. R., "Performance of Popular Turbulence Models for Attached and Separated Adverse Pressure Gradient Flows," AIAA Paper 91-1784, Honolulu, HI, 1991.

[14]Chen, Y. S., and Kim, S. W., "Computation of Turbulent Flows Using an Extended k-ϵ Closure Model," NASA CR-179204, Oct. 1987.